Rapid Communications

Fractional Chern insulator edges and layer-resolved lattice contacts

Christina Knapp,[1] Eric M. Spanton,[2] Andrea F. Young,[1] Chetan Nayak,[3,1] and Michael P. Zaletel[4,5]

[1]*Department of Physics, University of California, Santa Barbara, California 93106, USA*
[2]*California Nanosystems Institute, University of California, Santa Barbara, California 93106, USA*
[3]*Station Q, Microsoft Research, Santa Barbara, California 93106-6105, USA*
[4]*Department of Physics, University of California, Berkeley, California 94720, USA*
[5]*Department of Physics, Princeton University, Princeton, New Jersey 08540, USA*

(Received 19 November 2018; published 15 February 2019)

Fractional Chern insulators (FCIs) realized in fractional quantum Hall systems subject to a periodic potential are topological phases of matter for which space group symmetries play an important role. In particular, lattice dislocations in an FCI can host non-Abelian topological defects, known as genons. Genons can increase the ground-state degeneracy of the system and are thus potentially useful for topological quantum computing. In this work, we study FCI edges and how they can be used to detect genons. We find that translation symmetry can impose a quantized momentum difference between the edge electrons of a partially filled Chern band. We propose *layer-resolved lattice contacts*, which utilize this momentum difference to selectively contact a particular FCI edge electron. The relative current between FCI edge electrons can then be used to detect the presence of genons in the bulk FCI. Recent experiments have demonstrated graphene is a viable platform to study FCI physics. We describe how the lattice contacts proposed here could be implemented in graphene subject to an artificial lattice, thereby outlining a path forward for experimental dectection of non-Abelian topological defects.

DOI: 10.1103/PhysRevB.99.081114

Introduction. Non-Abelian topological physics has excited intense interest in the condensed-matter community, in part for its potential application to quantum computing [1,2]. Traditionally, the emphasis has been to discover non-Abelian topological phases, whose emergent quasiparticles are *non-Abelian anyons*. Non-Abelian anyons have an internal degenerate state space that can encode quantum information, and satisfy exotic braiding statistics such that their adiabatic exchange can result in a unitary rotation within the ground-state subspace. While more than three decades of searching for non-Abelian anyons has resulted in some progress [3–6], it has also emphasized the difficulty of conducting such experiments. An attractive alternative is to engineer extrinsic defects with non-Abelian braiding statistics and ground-state degeneracy. Such topological defects are potentially more experimentally manageable because their location and number can be controlled. Majorana zero modes (MZMs) in topological superconductors [7], defects with Ising anyon fusion and braiding statistics, have been the focus of these studies due to their relative experimental accessibility [8–20]. Unfortunately, the braiding statistics of MZMs do not support universal quantum computation [21], thus most MZM-based proposals rely on resource-expensive distillation protocols [22–27]. It therefore remains desirable to engineer alternative, more computationally powerful topological defects.

One potential alternative is genons—topological defects whose presence effectively changes the genus of the system [28–31]. Genons can increase the ground-state degeneracy of an otherwise Abelian topological phase, enhancing the computational power of the system. One system predicted to host genons is fractional Chern insulators (FCIs) [32–37]. An FCI is a topological phase occurring at partial filling of a band with nontrivial Chern number $C \in \mathbb{Z}/\{0\}$. The fractional quantum Hall (FQH) effect is a special case of an FCI, in which all bands (Landau levels) have $C = 1$. Applying a periodic potential (e.g., a lattice) to a QH system can result in bands with $|C| > 1$. The ground state of a partially filled Chern-C band can be mapped to a $|C|$-layer FQH state in which different lattice sites are analogous to layers [38–42]. Lattice symmetries are thus interwoven with internal component labels of the FCI; translations have a nontrivial action on layer index which can result in genons localized at lattice dislocations [40].

Recent experiments have demonstrated that FCIs can be realized in graphene, where the periodic potential arises from a moiré pattern formed by interference between the graphene and dielectric lattices [43]. These experiments indicate that graphene is a viable platform in which to pursue non-Abelian physics; however, the moiré potential is not readily applicable to genons as it is difficult to controllably insert lattice dislocations into the moiré superlattice. Alternatively, the lattice potential can be engineered, e.g., by patterning holes into a neighboring metallic gate or dielectric [44–46]. An artificial lattice is an appealing route toward realizing FCIs hosting genons because (1) the lattice itself can be used to tune to the desired phase, and (2) there is no additional cost associated with patterning dislocations.

Even after genons have been engineered, there remains a final hurdle of how to detect their presence, which is the focus of this work. To understand why this is challenging, consider the analogy of an FCI in a Chern-2 band to a bilayer QH system, depicted in Fig. 1. When the FCI ground state satisfies the microscopic lattice symmetries, sublattices are analogous to layers. Crucially, under this mapping, unit cell translations

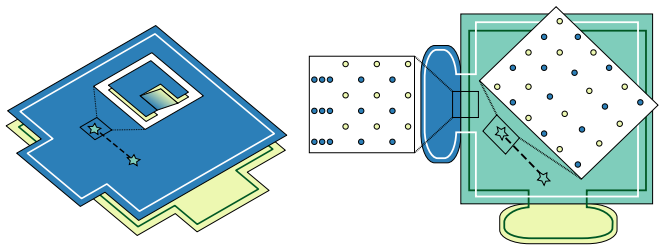

FIG. 1. Analogy between a bilayer QH system (left) and an FCI in a $C = 2$ band (right). Both systems contain a pair of genons (stars) and a blue and yellow region to selectively contact the two edge electrons (white and green lines). A genon in the bilayer system exchanges the layers. Right panel: An FCI (green) with two layer-resolved lattice contacts (blue and yellow). Each lattice contact gaps out one of the FCI's edge electrons, rerouting that electron along the exterior of the contact and allowing for selective voltage-bias and current measurement. The FCI is in a partially filled $C = 2$ band subject to a square lattice potential, such that it realizes the two-component (*mml*) phase. The two components, "layers," are localized on the blue and yellow sublattices. The contacts are in a $C = 1$ band. The unit cell area of the rectangular lattice is half that of the bulk, and is lattice matched with the bulk along the interface.

and plaquette-centered rotations interchange the two sublattices, therefore lattice dislocations play the same role as layer-exchange defects in the bilayer system. In the bilayer case, layer-exchange defects can be detected using the difference in the edge current of the two layers [47], which in turn can be measured by separately contacting each layer's edge. In the FCI case, the difference in the current associated with the edge electrons again carries a signature of the genon; however, we must devise a way to selectively contact edge electrons residing in the same physical sample.

In this work, we study FCI edges in a partially filled $C > 1$ band and propose *layer-resolved lattice contacts* that can be used to detect genons. The main idea is depicted in the left panel of Fig. 1. Essentially, translation symmetry along the edge constrains the allowed perturbations from electron tunneling between the FCI (green) and lattice contacts (blue/yellow). By appropriately designing the lattices in the three regions, the two contact interfaces can gap out different edge electrons of the FCI, thereby spatially separating them and allowing independent measurement of their electrical properties. The relative current can then be used to detect genons in the bulk [47], providing a path forward for experimental detection of non-Abelian topological defects in graphene.

The remainder of this Rapid Communication is organized as follows. We briefly review the mapping of an FCI ground state to a $|C|$-layer QH state. We next study the FCI edge physics, elucidating the additional constraints translation symmetry imposes on electron tunneling across the interface. We then discuss how the lattice itself can be used as a tuning parameter to simultaneously realize different phases in the same sample. Finally, we synthesize the above discussion to propose layer-resolved lattice contacts and illustrate how these contacts provide the missing link in experimental dectection of genons.

Preliminaries. Consider a square lattice with unit cell area a^2 and rational flux density $\phi = p/q$, with p and q coprime integers. Chern bands are characterized by topological invariants C and S given by the TKNN Diophantine equation [48]

$$n_e = C\phi + S, \tag{1}$$

where n_e is the electron density per unit cell. The single-particle orbitals of the band can be mapped to a $|C|$-layer QH system at flux density $\bar{\phi} = \phi + S/C$ with effective magnetic length $\bar{\ell}_B = a/\sqrt{2\pi\bar{\phi}}$ [49]. Recall that in the Landau gauge $\mathbf{A} = B(-y, 0)$ of a continuum Landau level, single-particle states are uniquely labeled by their momentum k_x. The key point is that in an appropriate basis, single-particle orbitals $|\tilde{k}_x, \beta\rangle$ of a Chern-C band have a continuum index $\tilde{k}_x \in \mathbb{R}$ analogous to this momentum, and an internal index $\beta \in \mathbb{Z}_C$ analogous to "layer." Translations and C_4 rotations factor into continuum and internal parts $T_j = \tilde{T}_j \otimes \tau_j$, $j = x, y$; $C_{4,l} = \tilde{C}_{4,l} \otimes \gamma_{4,l}$, $l = p, s$ denoting plaquette-centered and site-centered rotations, respectively ($C_{4,s} = T_x C_{4,p}$). The continuum parts, denoted with a tilde, transform $\tilde{k}_x$ just as in a continuum Landau level at flux density $\bar{\phi}$. When S and C are coprime, the internal parts, denoted with a greek letter, act nontrivially on the layer index: $\tau_x\tau_y = e^{2\pi i S/C}\tau_y\tau_x$. In the limit that $\bar{\phi} \to 0$, the system has a continuum limit and admits a field-theoretic description. This is the precise sense in which a Chern-C band is like a $|C|$-layer QH system, with lattice symmetries acting as internal symmetries on the layer index [38–42].

For concreteness, we consider a partially filled $C = 2$, S odd band whose ground state realizes an Abelian, C_4-symmetric (*mml*) state. At the topological level the system is described by the Lagrangian

$$\mathcal{L} = \frac{1}{4\pi}\int dx\{K_{IJ}a_{I,\mu}\partial_\nu a_{J,\nu}\varepsilon^{\mu\nu\lambda} + 2t_I A_\mu \partial_\nu a_{I,\lambda}\varepsilon^{\mu\nu\lambda}\}, \tag{2}$$

where K_{IJ} is a 2×2 universal matrix describing the phase, $\mathbf{t} = (1, 1)$ is the charge vector, $\mathbf{a}_J$ are the Chern-Simons gauge fields, and $\mathbf{A}$ is the external electromagnetic vector potential. The topological field theory must then be supplemented with the symmetry action. The electron current in layer I is $j^\mu_{e,I} = \frac{1}{2\pi}\partial_\nu a_{I,\lambda}\varepsilon^{\mu\nu\lambda}$, while the electron operator $\psi_{e,I}$ generates a corresponding flux in $\mathbf{a}_I$. We demand that the $\psi_{e,I}$ transform under the lattice symmetries just like the single-particle orbitals of a $C = 2$ band; specifically they transform under translations as $\tau_j = \sigma_j$ where $\sigma_{x/y}$ are Pauli matrices, and under rotations as $\gamma_{4,p} = (\tau_x + \tau_y)/\sqrt{2}$. This implicitly defines the action of the symmetry on the Chern-Simons fields, as detailed below. Note that by a change of basis in the layer space β, we could have instead chosen (say) $\tau_x = \sigma_z$; this corresponds to a *distinct* implementation of the symmetry (the "topological nematic" state of Ref. [28]). Our choice is C_4 symmetric. When $|m - l| \geqslant 2$, interchanging the layers permutes the anyons, and consequently [50] such twist defects are genons with quantum dimension $d = \sqrt{|m - l|}$ [28,40]. For $\tau_j = \sigma_j$, a lattice dislocation with a Burger's vector along *either* x or y permutes the layers, so will carry this degeneracy.

FCI edge states. The interplay of translation symmetry and the component labels of the many-body state has interesting implications for FCI edge states. The Lagrangian associated

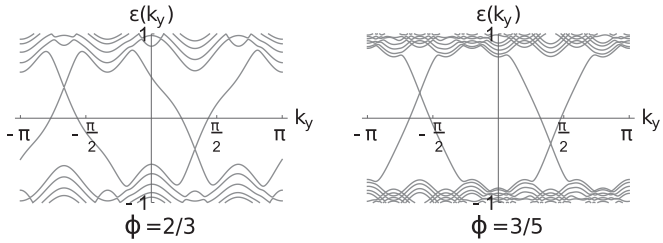

FIG. 2. Edge states for the Hofstadter model near $\phi = 1/2$ on the infinite cylinder. The two halves of the cylinder differ by filling a band with $C = 2$, $S = -1$, with left and right movers corresponding to opposite edges. The edge state momentum difference at $\varepsilon = 0$ is $\frac{\pi}{a}(1 + 1/q)$ for flux density p/q. As $p/q \to 1/2$, the edge state momentum difference approaches quantization, corresponding to the limit that the system admits a field theory description [49].

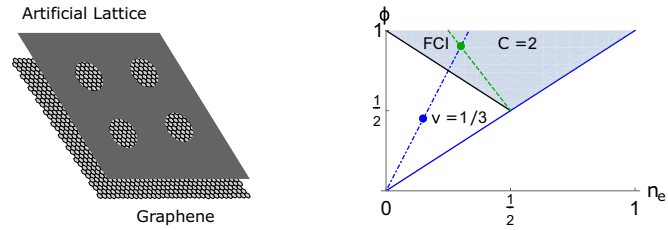

FIG. 3. Left panel: The FCI can be engineered in graphene subject to an artificial lattice, e.g., by patterning holes in a neighboring dielectric or metal gate [49]. Right panel: Flux density versus electron density phase space. The dot-dashed blue line corresponds to the FQH phase $\nu = 1/3$. The dashed green line corresponds to an FCI at quarter filling of a $C = 2$, $S = -1$ band (shaded region). The pair of points depict that for the different lattices shown in Fig. 1, the green and blue/yellow regions can be tuned to distinct phases for the same global backgate voltage and magnetic field.

with the edge of the system is [51]

$$\mathcal{L}_{\text{edge}} = \frac{1}{4\pi}\int dx\{K_{IJ}\partial_t\phi_I\partial_x\phi_J - V_{IJ}\partial_x\phi_I\partial_x\phi_J\}, \qquad (3)$$

where the matrix K_{IJ} is that of the bulk theory, while the edge potential V_{IJ} is nonuniversal. An edge along the (u, v) direction has translation symmetry $T_{(u,v)} = \tilde{T}_{(u,v)} \otimes \tau_{(u,v)}$. The "internal" part of the translation acts on electron operators $\psi_{e,I} \sim \exp\{iK_{IJ}\phi_J\}$ as $\tau_{(u,v)}(\psi_{e,1}, \psi_{e,2})^T$. For instance, in the (mml) phase an x edge $[(u, v) = (1, 0)]$ interchanges the bosonic modes: $\tau_x\phi_{1/2} = \phi_{2/1}$.

Translation symmetry imposes additional constraints on the allowed perturbations to Eq. (3). Consider a translationally invariant interface between two phases described by $K^{L/R}$. When these phases are not related by anyon condensation, only perturbations arising from electron tunneling across the interface are allowed. These perturbations take the form

$$t_{gh}\cos\left(g_I K^L_{IJ}\phi^L_J - h_I K^R_{IJ}\phi^R_J\right), \qquad (4)$$

where g_I and h_I are integer vectors satisfying $\sum_I g_I = \sum_I h_I$ from charge conservation. For QH systems, Eq. (4) can gap out the edge modes $e^{ig_I K^L_{IJ}\phi^L_J}$, $e^{ih_I K^R_{IJ}\phi^R_J}$ when the left and right scaling dimensions are equal and the total scaling dimension is less than two. For the FCI interface, Eq. (4) must additionally be invariant under the component translation symmetries of the left/right phases, $\tau^{L/R}_{(u,v)}$.

This additional constraint implies that the interplay of translation symmetry and layer index introduces an edge electron momentum difference that is not present for the analogous FQH state. Consider the (mml) state with $\tau_{x/y} = \sigma_{x/y}$. The (1,1) edge has $\tau_{(1,1)} = \sigma_z$. When V_{IJ} is a symmetric matrix, layer-exchange symmetry implies that the two edge electrons for a bilayer FQH state have the same momenta; this implies that for an FCI, both edge electrons $\psi_{e,1/2}$ have the same $\tilde{k}_{(1,1)}$. However, the *internal* part of the translation introduces a quantized momentum difference of $\pi/(\sqrt{2}a)$:

$$\tilde{T}_{(1,1)} \otimes \tau_{(1,1)}\begin{pmatrix}\psi_{e,1}\\ \psi_{e,2}\end{pmatrix} = e^{i\tilde{k}_{(1,1)}\sqrt{2}a}\begin{pmatrix}\psi_{e,1}\\ -\psi_{e,2}\end{pmatrix}. \qquad (5)$$

This momentum difference will no longer be quantized in the presence of nonsymmetric perturbations to V_{IJ}. Figure 2 shows this momentum difference approaches quantization in the limit $\phi \to -S/C$ for the Hofstadter model [52,53].

When the system satisfies plaquette-centered C_4 symmetry, the $(1, -1)$ edge has component translation $\tau_{(1,-1)} = \gamma^{-1}_{4,p}\tau_{(1,1)}\gamma_{4,p} = -\sigma_z$, and the momenta of the edge electrons are swapped compared to Eq. (5) (assuming $\tilde{k}_{(1,1)} = \tilde{k}_{(1,\pm1)}$). For the (331) state, there is an MZM at the corner, which interchanges the two layers of the FCI [49]. Due to the presence of gapless edge modes, these corner MZMs are not exponentially localized the way that topological defects in the gapped bulk are.

Lattice as a tuning parameter. We now focus on the particular realization of an FCI in graphene subject to an artificial lattice, depicted in Fig. 3. Insulating phases correspond to lines in the flux density ϕ versus electron density n_e plane [43]. The phase of the system can be tuned by (1) applying a voltage to the sample to vary n_e, (2) applying a perpendicular magnetic field to vary ϕ, and (3) changing the unit cell area of the lattice to change (n_e, ϕ) simultaneously. The third option provides a convenient way of realizing distinct phases within the same sample by defining the artificial lattice differently in separate spatial regions. We consider edges defined by the artificial lattice, as the physical graphene edge is too dirty.

Consider the right panel of Fig. 1: the unit cell area in the green region is twice as large as the unit cell area in the blue/yellow regions. Therefore, for the same magnetic field and backgate voltage, $2(n_e, \phi)_{\text{b/y}} = (n_e, \phi)_{\text{g}}$. When these points lie on lines characterizing distinct phases, the green and blue/yellow regions are in different phases. Figure 3 shows an example. The dashed green line corresponds to an FCI at quarter filling of a $C = 2$, $S = -1$ band (shaded region). A possible ground state of this phase is the Abelian (331) state, which hosts genons at lattice dislocations. The dot-dashed blue line corresponds to the FQH phase $\nu = 1/3$. When the green region is tuned to the point $(3/10, 9/10)$, the blue/yellow regions are at $(3/20, 9/20)$. Generally, for large ϕ FCI phases have larger energy gaps than competing FQH phases [43], therefore for these parameter values we would expect the bulk and lattice contacts to be in an FCI and FQH phase, respectively.

Layer-resolved lattice contacts. We now propose the layer-resolved lattice contacts shown in Fig. 1. We assume the bulk

(green) is in the plaquette-centered C_4-symmetric ground state of the (331) phase so that the layer basis corresponds to the blue and yellow sublattices (see insets). The two contacts (blue/yellow) are in the $\nu = 1/3$ phase. Possible parameter values for the bulk and contacts are given by the green and blue dots, respectively, in Fig. 3. Furthermore, we assume that the FCI-contact interface is sufficiently long that translation symmetry is preserved, and located in the middle of the edge so that corner physics may be neglected.

The white/green lines indicate the edge electrons $\psi_{e,1/2}$ associated with the FCI layer index. These electrons are eigenstates of the translation operators $T_{(1,\pm1)}$, and thus have well-defined momenta. The C_4 symmetry guarantees the momentum of $\psi_{e,1/2}$ along the yellow contact interface is equal to the momentum of $\psi_{e,2/1}$ along the blue contact interface. If the energy gaps of the (331) and $\nu = 1/3$ phases are compatible (i.e., the contact's edge electron has the same momentum as either $\psi_{e,1/2}$ for an appropriate value of the electrochemical potential), then $\psi_{e,1}$ and $\psi_{e,2}$ can be gapped out along opposite contacts. Reference [49] describes a tuning procedure for checking that the contact's edge electron has the necessary momentum. We do not show the edge electron associated with the filled $C = -1$ band (solid black line in Fig. 3); generically this edge electron's momentum will be different than that of the $\psi_{e,1/2}$ and does not change under C_4 rotation, thus it can be safely ignored. Effectively, gapping out an FCI's edge electron along the contact's interface reroutes that edge electron along the exterior of the contact, spatially separating the FCI's two edge electrons. A current measurement or voltage applied to the outer edge of the lattice contact will only affect one of the FCI's edge electrons, hence the name *layer-resolved lattice contacts*.

Given the ability to separately contact the two FCI edge electrons, we can use their relative current to detect genons localized at lattice dislocations in the bulk. Figure 4 generalizes an experimental proposal in Ref. [47] for a bilayer QH system with layer exchange defects. Let $I_{1/2}$ denote the current associated with $\psi_{e,1/2}$. The relative current $I_r = I_1 - I_2$ is inverted across a genon. The layer-resolved lattice contacts allow separate control of the voltage and measurement of the current for the two edge electrons, thereby allowing readout of their relative conductance, dI_r/dV_r. The relative conductance peaks for small edge-genon separation; therefore by comparing multiple samples that vary this separation distance, we can obtain spatial resolution of the relative conductance and detect the genon. The quantum point contact interferometer of Ref. [47] can be similarly generalized to the FCI context.

There are many other choices for the FCI and lattice contact phases; the two phases can be realized simultaneously for constant magnetic field and backgate voltage provided the line connecting $(n_e, \phi)_{\rm g}$ and $(n_e, \phi)_{\rm b/y}$ intersects the origin. In Ref. [49], we propose an alternate realization of the experiment in Fig. 4 for an FCI-contact interface along the (1,0) direction. Finally, while we focused here on a C_4-symmetric FCI, the proposal could be generalized to other lattices.

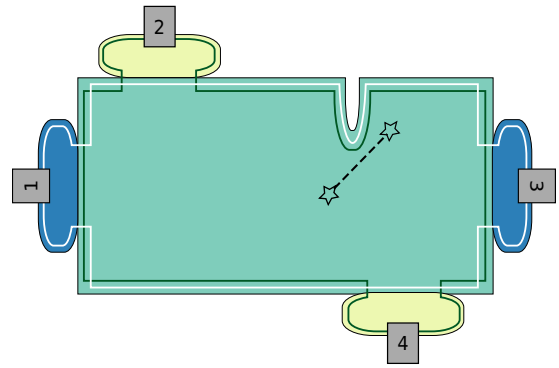

FIG. 4. Detecting genons using FCI edges. The two edge electrons (white/green lines) are interchanged at a genon (star), resulting in a signature in the differential conductance dI_r/dV_r [47]. When all contacts are held to the same chemical potential, electrodes 1 and 3 selectively couple to one of the FCI's edge electrons, while 2 and 4 couple to the other. By measuring the voltage drop between 1 and 3, as well as 2 and 4, we can determine the relative current I_r. The differential conductance dI_r/dV_r can then be determined by varying the voltage applied to any of the four electrodes.

Summary and outlook. In this work, we proposed layer-resolved lattice contacts for FCI edges. The lattice contacts utilize the interplay of translation symmetry with internal component labels of the FCI state to selectively couple to one of the FCI's edge electrons. Lattice contacts facilitate genon detection in the bulk by measuring the differential conductance associated with the relative current between the edge electrons, which in our proposal becomes a standard four-terminal conductance measurement. The experimental proposal in this Rapid Communication could be realized using graphene subject to an artificial lattice.

For the (331) phase, the genons are MZMs; more exotic topological defects are possible for (mml) phases with $|m - l| > 2$ [28]. Open questions include determining the energy gaps, ground states, and symmetries, of fractionally filled Chern bands. Additionally, the role of disorder, and whether it causes FCI edge modes to equilibrate, could affect our proposal. More broadly, FCIs realized with an artificial lattice provide a playground for studying interfaces of different topological phases, including the transfer and sharing of information across the interface.

Acknowledgments. C.K. acknowledges support from the NSF GRFP under Grant No. DGE 114085. E.M.S. and A.F.Y. were supported by the National Science Foundation under EAGER Grant No. DMR-1836776. E.M.S. acknowledges the support of the Elings Fellowship from the California NanoSystems Institute at the University of California, Santa Barbara. A.F.Y. acknowledges the support of the David and Lucile Packard Foundation 2016-65145.

[1] A. Y. Kitaev, Fault-tolerant quantum computation by anyons, Ann. Phys. (NY) **303**, 2 (2003).

[2] C. Nayak, S. H. Simon, A. Stern, M. Freedman, and S. Das Sarma, Non-Abelian anyons and topological quantum computation, Rev. Mod. Phys. **80**, 1083 (2008).

[3] M. Dolev, M. Heiblum, V. Umansky, A. Stern, and D. Mahalu, Observation of a quarter of an electron charge at the $\nu = 5/2$ quantum Hall state, Nature (London) **452**, 829 (2008).

[4] I. P. Radu, J. B. Miller, C. M. Marcus, M. A. Kastner, L. N. Pfeiffer, and K. W. West, Quasi-particle properties from

tunneling in the $\nu = 5/2$ fractional quantum Hall state, Science **320**, 899 (2008).

[5] R. L. Willett, L. N. Pfeiffer, and K. W. West, Alternation and interchange of e/4 and e/2 period interference oscillations consistent with filling factor 5/2 non-Abelian quasiparticles, Phys. Rev. B **82**, 205301 (2010).

[6] M. Banerjee, M. Heiblum, V. Umansky, D. E. Feldman, Y. Oreg, and A. Stern, Observation of half-integer thermal Hall conductance, Nature **559**, 205 (2018).

[7] A. Y. Kitaev, Unpaired majorana fermions in quantum wires, Phys. Usp. **44**, 131 (2001).

[8] R. M. Lutchyn, J. D. Sau, and S. Das Sarma, Majorana Fermions and a Topological Phase Transition in Semiconductor-Superconductor Heterostructures, Phys. Rev. Lett. **105**, 077001 (2010).

[9] Y. Oreg, G. Refael, and F. von Oppen, Helical Liquids and Majorana Bound States in Quantum Wires, Phys. Rev. Lett. **105**, 177002 (2010).

[10] J. Alicea, New directions in the pursuit of majorana fermions in solid state systems, Rep Prog. Phys. **75**, 076501 (2012).

[11] V. Mourik, K. Zuo, S. M. Frolov, S. R. Plissard, E. P. A. M. Bakkers, and L. P. Kouwenhoven, Signatures of Majorana fermions in hybrid superconductor-semiconductor nanowire devices, Science **336**, 1003 (2012).

[12] L. P. Rokhinson, X. Liu, and J. K. Furdyna, The fractional a.c. Josephson effect in a semiconductor-superconductor nanowire as a signature of Majorana particles, Nat. Phys. **8**, 795 (2012).

[13] A. D. K. Finck, D. J. Van Harlingen, P. K. Mohseni, K. Jung, and X. Li, Anomalous Modulation of a Zero-Bias Peak in a Hybrid Nanowire-Superconductor Device, Phys. Rev. Lett. **110**, 126406 (2013).

[14] A. Das, Y. Ronen, Y. Most, Y. Oreg, M. Heiblum, and H. Shtrikman, Zero-bias peaks and splitting in an Al-InAs nanowire topological superconductor as a signature of Majorana fermions, Nat. Phys. **8**, 887 (2012).

[15] M. T. Deng, C. L. Yu, G. Y. Huang, M. Larsson, P. Caroff, and H. Q. Xu, Anomalous zero-bias conductance peak in a Nb–InSb nanowire-Nb hybrid device, Nano Lett. **12**, 6414 (2012).

[16] H. O. H. Churchill, V. Fatemi, K. Grove-Rasmussen, M. T. Deng, P. Caroff, H. Q. Xu, and C. M. Marcus, Superconductor-nanowire devices from tunneling to the multichannel regime: Zero-bias oscillations and magnetoconductance crossover, Phys. Rev. B **87**, 241401 (2013).

[17] S. Nadj-Perge, I. K. Drozdov, J. Li, H. Chen, S. Jeon, J. Seo, A. H. MacDonald, B. A. Bernevig, and A. Yazdani, Observation of majorana fermions in ferromagnetic atomic chains on a superconductor, Science **346**, 602 (2014).

[18] S. M. Albrecht, A. P. Higginbotham, M. Madsen, F. Kuemmeth, T. S. Jespersen, J. Nygård, P. Krogstrup, and C. M. Marcus, Exponential protection of zero modes in Majorana islands, Nature (London) **531**, 206 (2016).

[19] H. Zhang, C.-X. Liu, S. Gazibegovic, D. Xu, J. A. Logan, G. Wang, N. van Loo, J. D. S. Bommer, M. W. A. de Moor, D. Car, R. L. M. Op Het Veld, P. J. van Veldhoven, S. Koelling, M. A. Verheijen, M. Pendharkar, D. J. Pennachio, B. Shojaei, J. S. Lee, C. J. Palmstrøm, E. P. A. M. Bakkers, S. D. Sarma, and L. P. Kouwenhoven, Quantized Majorana conductance, Nature (London) **556**, 74 (2018).

[20] R. M. Lutchyn, E. P. A. M. Bakkers, L. P. Kouwenhoven, P. Krogstrup, C. M. Marcus, and Y. Oreg, Majorana zero modes in superconductor-semiconductor heterostructures, Nat. Rev. Mater. **3**, 52 (2018).

[21] D. Gottesman, The Heisenberg representation of quantum computers, arXiv:quant-ph/9807006.

[22] S. Bravyi and A. Kitaev, Universal quantum computation with ideal Clifford gates and noisy ancillas, Phys. Rev. A **71**, 022316 (2005).

[23] S. Bravyi, Universal quantum computation with the $\nu = 5/2$ fractional quantum Hall state, Phys. Rev. A **73**, 042313 (2006).

[24] S. Bravyi and J. Haah, Magic state distillation with low overhead, Phys. Rev. A **86**, 052329 (2012).

[25] G. Duclos-Cianci and K. M. Svore, Distillation of nonstabilizer states for universal quantum computation, Phys. Rev. A **88**, 042325 (2013).

[26] J. Haah, M. B. Hastings, D. Poulin, and D. Wecker, Magic state distillation with low space overhead and optimal asymptotic input count, Quantum **1**, 31 (2017).

[27] J. Haah, M. B. Hastings, D. Poulin, and D. Wecker, Magic state distillation at intermediate size, Quantum Inf. Comput. **18**, 0114 (2018).

[28] M. Barkeshli, C.-M. Jian, and X.-L. Qi, Twist defects and projective non-Abelian braiding statistics, Phys. Rev. B **87**, 045130 (2013).

[29] M. Barkeshli and J. D. Sau, Physical architecture for a universal topological quantum computer based on a network of Majorana nanowires, arXiv:1509.07135.

[30] M. Barkeshli and M. Freedman, Modular transformations through sequences of topological charge projections, Phys. Rev. B **94**, 165108 (2016).

[31] I. Cong, M. Cheng, and Z. Wang, On defects between gapped boundaries in two-dimensional topological phases of matter, Phys. Rev. B **96**, 195129 (2017).

[32] F. D. M. Haldane, Model for a Quantum Hall Effect without Landau Levels: Condensed-Matter Realization of the "Parity Anomaly," Phys. Rev. Lett. **61**, 2015 (1988).

[33] N. Regnault and B. A. Bernevig, Fractional Chern Insulator, Phys. Rev. X **1**, 021014 (2011).

[34] T. Neupert, L. Santos, S. Ryu, C. Chamon, and C. Mudry, Fractional topological liquids with time-reversal symmetry and their lattice realization, Phys. Rev. B **84**, 165107 (2011).

[35] S. A. Parameswaran, R. Roy, and S. L. Sondhi, Fractional quantum Hall physics in topological flat bands, C. R. Phys. **14**, 816 (2013).

[36] E. J. Bergholtz and Z. Liu, Topological flat band models and fractional Chern insulators, Int. J. Mod. Phys. B **27**, 1330017 (2013).

[37] G. Möller and N. R. Cooper, Fractional Chern Insulators in Harper-Hofstadter Bands with Higher Chern Number, Phys. Rev. Lett. **115**, 126401 (2015).

[38] X.-L. Qi, Generic Wave-Function Description of Fractional Quantum Anomalous Hall States and Fractional Topological Insulators, Phys. Rev. Lett. **107**, 126803 (2011).

[39] Y.-L. Wu, N. Regnault, and B. A. Bernevig, Gauge-fixed Wannier wave functions for fractional topological insulators, Phys. Rev. B **86**, 085129 (2012).

[40] M. Barkeshli and X.-L. Qi, Topological Nematic States and Non-Abelian Lattice Dislocations, Phys. Rev. X **2**, 031013 (2012).

[41] F. Harper, S. H. Simon, and R. Roy, Perturbative approach to flat Chern bands in the Hofstadter model, Phys. Rev. B **90**, 075104 (2014).

[42] M. Ippoliti, M. Cheng, and M. P. Zaletel (unpublished).

[43] E. M. Spanton, A. A. Zibrov, H. Zhou, T. Taniguchi, K. Watanabe, M. P. Zaletel, and A. F. Young, Observation of fractional Chern insulators in a van der Waals heterostructure, Science **360**, 62 (2018).

[44] C. Albrecht, J. H. Smet, K. von Klitzing, D. Weiss, V. Umansky, and H. Schweizer, Evidence of Hofstadter's Fractal Energy Spectrum in the Quantized Hall Conductance, Phys. Rev. Lett. **86**, 147 (2001).

[45] T. Hensgens, U. Mukhopadhyay, P. Barthelemy, S. Fallahi, G. C. Gardner, C. Reichl, W. Wegscheider, M. J. Manfra, and L. M. K. Vandersypen, Capacitance spectroscopy of gate-defined electronic lattices, arXiv:1709.09058.

[46] C. Forsythe, X. Zhou, T. Taniguchi, K. Watanabe, A. Pasupathy, P. Moon, M. Koshino, P. Kim, and C. R. Dean, Band structure engineering of 2D materials using patterned dielectric superlattices, Nat. Nanotechnol. **13**, 566 (2018).

[47] M. Barkeshli and X.-L. Qi, Synthetic Topological Qubits in Conventional Bilayer Quantum Hall Systems, Phys. Rev. X **4**, 041035 (2014).

[48] D. J. Thouless, M. Kohmoto, M. P. Nightingale, and M. den Nijs, Quantized Hall Conductance in a Two-Dimensional Periodic Potential, Phys. Rev. Lett. **49**, 405 (1982).

[49] See Supplemental Material at http://link.aps.org/supplemental/10.1103/PhysRevB.99.081114 for more details on the mapping to a $|C|$-component QH system, edge momenta separation, corner MZMs, and experimental proposal.

[50] M. Cheng, M. Zaletel, M. Barkeshli, A. Vishwanath, and P. Bonderson, Translational Symmetry and Microscopic Constraints on Symmetry-Enriched Topological Phases: A View from the Surface, Phys. Rev. X **6**, 041068 (2016). .

[51] X.-G. Wen, Theory of the edge states in fractional quantum Hall effects, Int. J. Mod. Phys. B **06**, 1711 (1992).

[52] D. R. Hofstadter, Energy levels and wave functions of Bloch electrons in rational and irrational magnetic fields, Phys. Rev. B **14**, 2239 (1976).

[53] P. G. Harper, The general motion of conduction electrons in a uniform magnetic field, with application to the diamagnetism of metals, Proc. Phys. Soc., London, Sect. A **68**, 879 (1955).